Rev Esp Cardiol. 2023;76(5):301–311

Original article

ROD2 domain filamin C missense mutations exhibit a distinctive cardiac phenotype with restrictive/hypertrophic cardiomyopathy and saw-tooth myocardium

Francisco José Bermúdez-Jiménez,[a,b] Víctor Carriel,[c] Juan José Santos-Mateo,[d,e,f] Adrián Fernández,[g] Soledad García-Hernández,[h] Karina Analía Ramos,[i] Jesús Piqueras-Flores,[j] Eva Cabrera-Romero,[k,e] Roberto Barriales-Villa,[l] Luis de la Higuera Romero,[h] Juan Emilio Alcalá López,[a] Juan Ramón Gimeno Blanes,[d,e,f] David Sánchez-Porras,[c] Fernando Campos,[c] Miguel Alaminos,[c] José Manuel Oyonarte-Ramírez,[a] Miguel Álvarez,[a] Luis Tercedor,[a] Andreas Brodehl,[m] and Juan Jiménez-Jáimez[a,*]

[a] *Servicio de Cardiología, Hospital Universitario Virgen de las Nieves, Instituto de Investigación Biosanitaria ibsGRANADA, Granada, Spain*
[b] *Centro Nacional de Investigaciones Cardiovasculares Carlos III (CNIC), Madrid, Spain*
[c] *Departamento de Histología, Grupo de Ingeniería Tisular, Universidad de Granada, Instituto de Investigación Biosanitaria ibsGRANADA, Granada, Spain*
[d] *Servicio de Cardiología, Hospital Universitario Virgen de la Arrixaca, Instituto Murciano de Investigación Biosanitaria Virgen de la Arrixaca Murcia (IMIB), Murcia, Spain*
[e] *Centro de Investigación Biomédica en Red de Enfermedades Cardiovasculares (CIBERCV), Spain*
[f] *European Reference Network for Rare and Low Prevalence Complex Diseases of the Heart (ERN-Guard Heart), Amsterdam, Netherlands*
[g] *Servicio de Cardiología, Hospital Universitario Fundación Favaloro, Buenos Aires, Argentina*
[h] *Health in Code SL, Cardiología y Departamento Científico, Instituto de Investigación Biomédica de A Coruña (INIBIC), A Coruña, Spain*
[i] *Servicio de Cardiología, Hospital Centenario, Facultad de Ciencias Médicas, Universidad de Rosario, Argentina*
[j] *Servicio de Cardiología, Hospital General Universitario de Ciudad Real, Ciudad Real, Spain*
[k] *Servicio de Cardiología, Hospital Universitario Puerta de Hierro-Majadahonda, Majadahonda, Madrid, Spain*
[l] *Complexo Hospitalario Universitario A Coruña, Instituto de Investigación Biomédica de A Coruña (INIBIC), A Coruña, Spain*
[m] *Erich and Hanna Klessmann Institute for Cardiovascular Research & Development (EHKI), Heart and Diabetes Center NRW, University Hospital of the Ruhr-University Bochum, Bad Oeynhausen, Germany*

Article history:
Received 31 January 2022
Accepted 28 July 2022
Available online 8 August 2022

Keywords:
Filamins
Cardiomyopathies
Cardiomyopathy
Restrictive
Cardiomyopathies
Hypertrophic
Filamin C
Saw-tooth myocardium

ABSTRACT

Introduction and objectives: Missense mutations in the filamin C (*FLNC*) gene have been reported as cause of inherited cardiomyopathy. Knowledge of the pathogenicity and genotype-phenotype correlation remains scarce. Our aim was to describe a distinctive cardiac phenotype related to rare missense *FLNC* variants in the ROD2 domain.

Methods: We recruited 21 unrelated families genetically evaluated because of hypertrophic cardiomyopathy (HCM)/restrictive cardiomyopathy (RCM) phenotype carrying rare missense variants in the ROD2 domain of *FLNC* (*FLNC*-mRod2). Carriers underwent advanced cardiac imaging and genetic cascade screening. Myocardial tissue from 3 explanted hearts of a missense *FLNC* carrier was histologically analyzed and compared with an *FLNC*-truncating variant heart sample and a healthy control. Plasmids independently containing 3 *FLNC* missense variants were transfected and analyzed using confocal microscopy.

Results: Eleven families (52%) with 20 assessed individuals (37 [23.7-52.7]) years showed 15 cases with a cardiac phenotype consisting of an overlap of HCM-RCM and left ventricular hypertrabeculation (saw-tooth appearance). During a median follow-up of 6.49 years, they presented with advanced heart failure: 16 (80%) diastolic dysfunction, 3 heart transplants, 3 heart failure deaths) and absence of cardiac conduction disturbances or skeletal myopathy. A total of 6 families had moderate genotype-phenotype segregation, and the remaining were *de novo* variants. Differential extracellular matrix remodeling and *FLNC* distribution among cardiomyocytes were confirmed on histology. HT1080 and H9c2 cells did not reveal cytoplasmic aggregation of mutant *FLNC*.

Conclusions: *FLNC*-mRod2 variants show a high prevalence of an overlapped phenotype comprising RCM, HCM and deep hypertrabeculation with saw-tooth appearance and distinctive cardiac histopathological remodeling.

* Corresponding author.
E-mail address: jimenez.jaimez@gmail.com (J. Jiménez-Jáimez).
@ArritmiasGr

https://doi.org/10.1016/j.rec.2022.08.002
1885-5857/

Las mutaciones *missense* en el dominio ROD2 de la filamina C muestran un fenotipo con miocardiopatía restrictiva/hipertrófica y miocardio en dientes de sierra

Palabras clave:
Filaminas
Miocardiopatía
Cardiomiopatía restrictiva
Cardiomiopatía Hipertrófica
Filamina C
Miocardio en dientes de sierra

RESUMEN

Introducción y objetivos: Recientemente se han descrito mutaciones *missense* en la filamina C (FLNC) como causa de miocardiopatía. Los conocimientos sobre la patogenicidad y la correlación genotipo-fenotipo son escasos. Nuestro objetivo es describir un fenotipo cardiaco distintivo relacionado con mutaciones *missense* en el dominio ROD2 de FLNC (FLNC-mRod2).

Métodos: Incluimos 21 familias independientes con fenotipo de miocardiopatía hipertrófica (MCH)/miocardiopatía restrictiva (MCR) portadoras de variantes *missense* en FLNC-mRod2. Se estudió clínicamente a los portadores, además de hacer un cribado en cascada. Se analizó histológicamente el tejido miocárdico de tres corazones explantados y se comparó con un corazón portador de un truncamiento de FLNC y con un control sano. Se transfectaron plásmidos con mutaciones *missense* de FLNC y se analizaron mediante microscopía confocal.

Resultados: En 11 familias (52%) con 20 individuos evaluados (37 [23,7-52,7] años), 15 casos presentaron un fenotipo cardiaco consistente en una superposición de MCH-MCR e hipertrabeculación ventricular izquierda (apariencia de dientes de sierra). Durante una mediana de seguimiento de 6,49 años presentaron principalmente insuficiencia cardiaca avanzada (16 (80%) disfunción diastólica, 3 trasplantes cardiacos, 3 muertes por insuficiencia cardiaca) en ausencia de alteraciones de la conducción cardiaca o miopatía esquelética. Un total de 6 familias presentaban segregación genotipo-fenotipo leve, y las restantes eran mutaciones *de novo*. Se observó una remodelación de la matriz extracelular y distribución de la FLNC diferencial en los cardiomiocitos. Las células HT1080 y H9c2 no revelaron agregados citoplasmáticos de FLNC.

Conclusiones: Las variantes en FLNC-mRod2 exhiben una alta prevalencia de fenotipo solapado de MCR, MCH e hipertrabeculación en dientes de sierra, con una remodelación histopatológica cardiaca distintiva.

Abbreviations

FLNC: filamin C
HCM: hypertrophic cardiomyopathy
HF: heart failure
LVHT: left ventricular hypertrabeculation
NCCM: noncompaction cardiomyopathy
RCM: restrictive cardiomyopathy

INTRODUCTION

The increasing availability of next-generation sequencing technology has led to the important insight that cardiomyopathies are genetically heterogeneous disorders with different expressivity and penetrance. In most cardiomyopathies, the genotype-phenotype mechanisms within the same mutant gene remain widely unknown.

The *FLNC* gene encodes the main cardiac protein filamin C (*FLNC*), expressed in striated muscle cells, interacting with several proteins at Z-disk of the sarcomeres and with structural and signaling functions in the cardiomyocyte. The gene contains an actin-binding region, 2 hinge regions and a domain with 24 Ig-like repeats. *FLNC* plays a role in myogenesis, preserving myofibrils and sarcomere ultrastructure. Moreover, *FLNC* acts as an anchor membrane protein to the structural cytoskeletal proteins.[1,2]

Classically, *FLNC* mutations have been associated with a spectrum of inherited muscular diseases known as myofibrillar myopathies.[3] In the last decade, a few reports based on a limited number of patients have described *FLNC* missense variants causing inherited restrictive cardiomyopathy (RCM),[4–6] hypertrophic cardiomyopathy (HCM),[7] or noncompaction cardiomyopathy (NCCM)[8] with nearly absent skeletal muscle involvement. More recently, several studies have reported truncating variants in *FLNC* (*FLNC*-tv) related to arrhythmogenic cardiomyopathy.[9,10] Despite being an increasingly recognized genetic cause of inherited cardiomyopathy, the causative relationship between *FLNC* missense variants and overlapped cardiac phenotypes is not clearly established.

Our aim was to describe phenotypic features of cardiomyopathy related to missense *FLNC* variants in the ROD2 domain (*FLNC*-mRod2).

METHODS

Study population and clinical evaluation

We collected all probands referred for cardiovascular genetic evaluation at the same reference laboratory because HCM or RCM showing an *FLNC*-mRod2 variant, and who were available for study. We excluded all individuals with another causative variant to explain the phenotype. After the first evaluation, we selected those families with saw-tooth appearance at cardiovascular imaging for an in-depth clinical study.

We performed a comprehensive clinical assessment including a detailed evaluation of the patient's clinical history, pedigree, creatine kinase, 12-lead electrocardiogram, Holter monitoring, and expert echocardiography assessment. Left ventricular ejection fraction dysfunction was assessed by the Simpson biplane method.[11] Diastolic function was evaluated according to current recommendations.[12] Left ventricle (LV) myocardium appearance was analyzed with a special focus on hypertrabeculation, according to current diagnostic criteria for NCCM with 2 well-defined layers (thin compacted and thick noncompacted layers).[13] Saw-tooth myocardium was identified as the presence of multiple deep projections and invaginations in a dense and compacted myocardium.

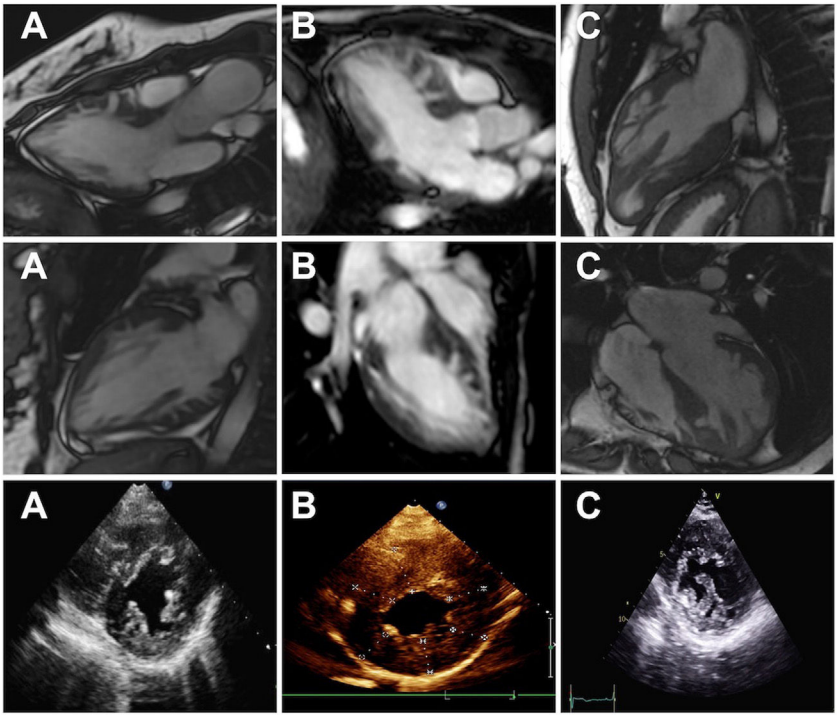

Figure 1. Cardiac magnetic resonance (top and center panels) and echocardiogram (lower panel) images showing the saw-tooth left ventricular hypertrabeculation appearance with muscular projections and deep crypts distorting the normal left ventricular architecture. A, patient III.1 from family C; B, patient II.2 from family A; C, patient from family E.

The study was approved by the local ethics committee. Informed written consent for inclusion in the study was obtained from all participants or, in the case of minors or deceased individuals, from first-degree family members.

Genetic sequencing

Blood samples from probands were obtained for genetic sequencing using a phenotype-guided next-generation sequencing panel at the same institution. In probands with an overlap or nondefined phenotype, we used a next-generation sequencing panel including genes related or candidates for cardiac disease. Coding exons and intronic boundaries of 247 genes related to inherited cardiovascular diseases (table 1 of the supplementary data) were captured using a custom probe library.

For the pathogenicity assessment of genetic variants, we considered information such as frequency in public databases (eg, the Human Gene Mutation Database the Single Nucleotide Polymorphism Database, NHLBI GO Exome Sequencing Project and ClinVar or in the Genome Aggregation Database,[14–16] its previous description in the literature and preservation among species. After identification of rare *FLNC* variants in the index patients, we performed a genetic cascade screening among all available relatives using Sanger DNA sequencing. For the *de novo* variants, paternity was confirmed when available. Finally, the logarithm of the odds score[17] and American College of Medical Genetics and Genomics (ACMG)[18] classification were evaluated. For detailed methods regarding the genetic analysis see supplementary data.

Histological evaluation

A complete histological, histochemical and immunohistochemical characterization of cardiac tissue belonging to 3 explanted hearts (patient from family F and family C, patients 2 and 3) was performed. Tissue samples were fixed for at least 48 hours in 10% neutral buffered formaldehyde, washed, dehydrated in ascending concentration of ethanol, cleared in xylol, and finally embedded in paraffin following a conventional protocol.[19]

Histological section of 5 μm thickness were obtained, dewaxed, hydrated and underwent the following steps: *a)* general histological examination was conducted with hematoxylin-eosin; *b)* the cardiomyocytes myofibrils were histochemical stained with Heidenhain hematoxylin; *c)* the organization and distribution of the main extracellular matrix (ECM) components were evaluated by Picrocirius collagen staining, Gomori's metal reduction technique for reticular fibers, Orcein histochemical staining for elastic fibers, and Alcian Blue staining for proteoglycans. In addition, collagens type I and IV (COL-I and COL-IV respectively) were identified by immunohistochemistry; *d)* the distribution pattern of *FLNC* and connexin-43 (Cx-43) were determined by immunohistochemistry. Technical details of the antibodies used are summarized in table 2 of the supplementary data.

In addition to the histological characterization, a semiquantitative analysis of the cell/collagen ECM area ratio was carried out in 3 different sections from 3 different tissue slides stained with the Picrocirius technique by using Image J software (National Institute of Health, United States) and following a previously described procedure.[20] Furthermore, 20 points were selected in 3 sections from each condition stained with the Heidenhain hematoxylin method and the intensity of the histochemical reaction for myofibrils was determined. Finally, the cell width was calculated in 20 cells per image selected in 3 images from each condition.

To detect specific histological changes attributable to *FLNC*-mRod2 variants, we compared the histological findings with a nonpathological heart tissue sample (control), and with an *FLNC*-truncating variant (*FLNC*-tv) carrier sample from our historical cohort. The *FLNC-tv* case showed the recognized overlapping

phenotype of dilated cardiomyopathy and arrhythmogenic cardiomyopathy.[9,10]

Plasmid generation, cell culture, and confocal microscopy

The wild-type plasmid pCMV6-*FLNC* (212462; OriGene Technologies, United States) was used as a template to insert the variants p.P2301L, p.E3224K and p.R2340W using the Quik Change Lightning Kit (Agilent Technologies, United States) in combination with appropriate oligonucleotides (table 3 of the supplementary data). The *FLNC* encoding complementary deoxyribonucleic acid (cDNA) of all plasmids was verified by Sanger sequencing (Macrogen, Netherlands). HT1080 (DSMZ, German Collection of Microorganisms and Cell Culture, ACC315, Germany) and H9C2 cells (ATCC, CRL-1446, United States) were cultured in μSlide chambers (ibidi GmbH, Germany) using Dulbecco's Modified Eagle Medium supplemented with 10% fetal calf serum and penicillin/streptomycin. Lipofectamin 3000 (Thermo Fisher Scientific, United States) was used for cell transfection according to the manufacturer's instructions. Twenty-four hours after transfection, cells were washed with phosphate buffered saline and were fixed for 10 minutes at room temperature using 4% Histofix (Carl-Roth, Germany). Immunocytochemistry analysis was performed as recently described using the TCS SP8 confocal microscope (Leica Microsystems, Germany).[4]

Statistical analysis

Statistical analyses were conducted using SPSS Statistics software, version 21.0. (IBM Corp, United States). Continuous variables are reported as mean value ± standard deviation for each measurement. For quantification of histological variables, we performed the Mann-Whitney *U* test (nonparametric). All categorical variables are expressed as frequencies and percentages.

RESULTS

Patients' characteristics

In total, we recruited 21 unrelated families from 7 reference centers who were genetically tested for HCM/RCM and found to carry rare *FLNC*-mRod2 variants (figure 1 of the supplementary data). A total of 11 families (52%) with 20 individuals (37 [23.7-

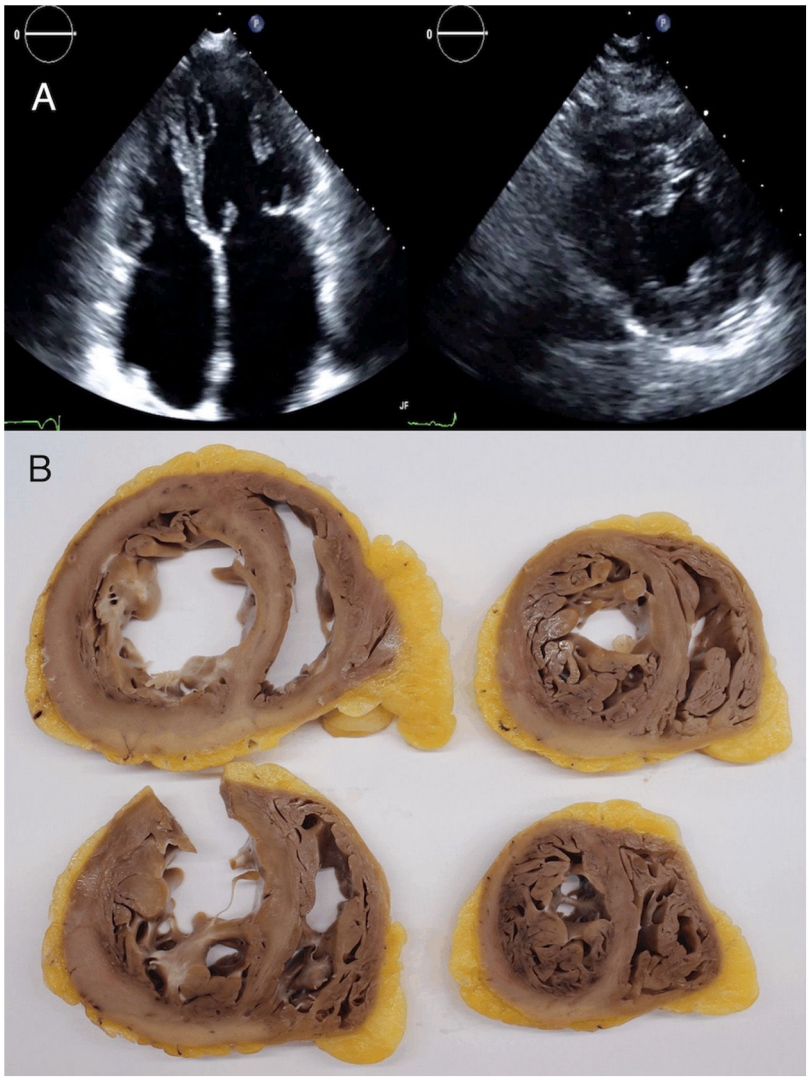

Figure 2. Echocardiogram images (A) and macroscopic images of explanted heart (B) from the index patient of family C, aged 24 and 36 years, respectively. Echocardiogram images showed left ventricular muscular protrusions. Pathological images showed the atypical and marked hypertrabeculation with profound recesses.

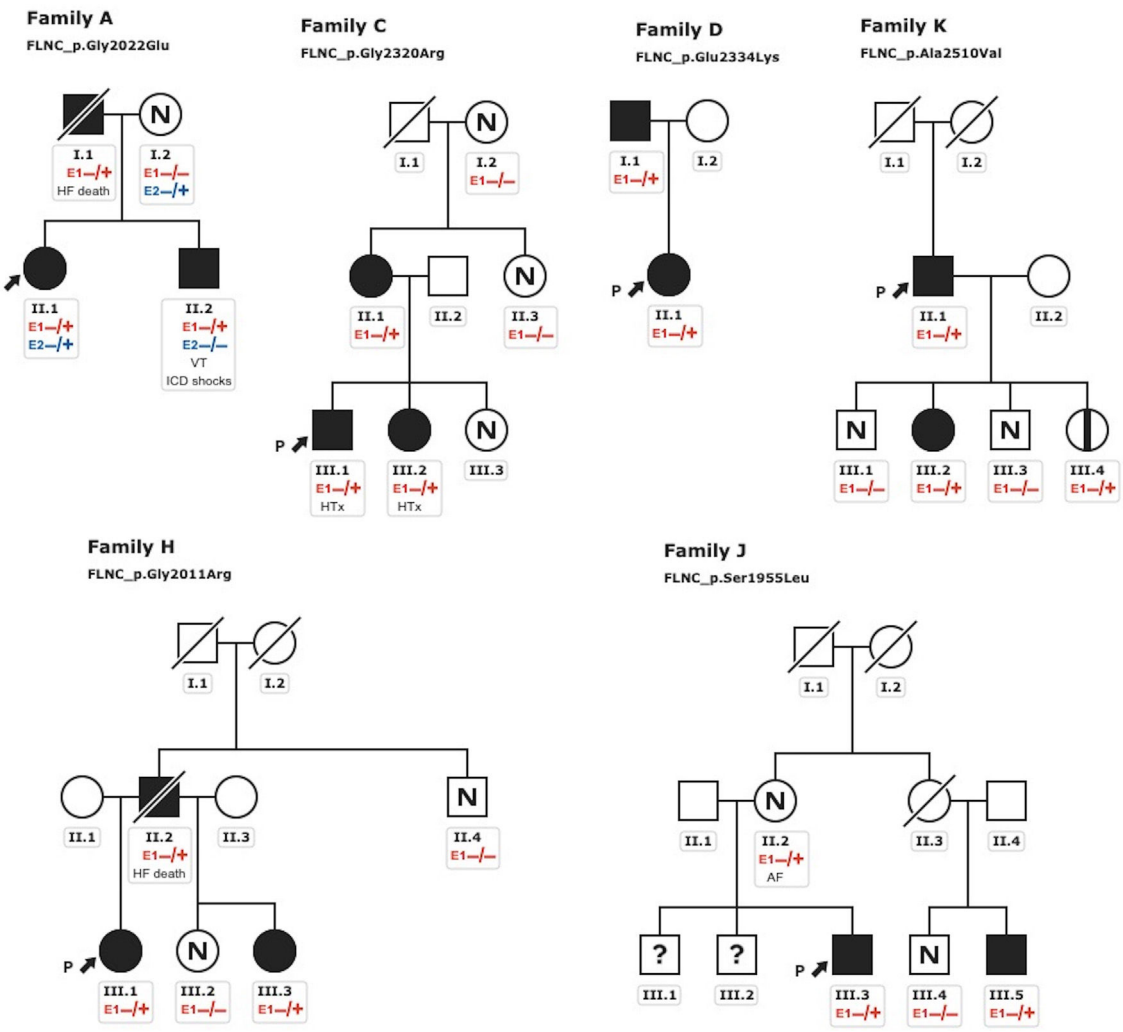

Figure 3. Pedigrees of families with mild cosegregation. Squares indicate males, circles indicate females, slashes indicate deceased individuals, black shading indicates cardiomyopathy phenotype, black stripe indicates silent carrier, N indicates absence of phenotype, (?) indicates not available for evaluation. The arrows + P indicate the proband. Heterozygous carriers (E1 —/+) and noncarriers (E1 —/—). ICD, implantable cardioverter-defibrillator; HF, heart failure; HTx, heart transplant; VT, sustained ventricular tachycardia.

52.7] years) showed 15 cases with a cardiac phenotype consisting of HCM or RCM with a marked and atypical left ventricular hypertrabeculation (LVHT) distorting LV with the presence of numerous cross bridging muscular projections. These protrusions of muscular bridges in the LV delineated deep crypts in a single, dense, and compacted myocardium (figure 1), which we have identified as "saw-tooth" appearance, different from the 2 characteristic layers of the NCCM (thin compacted and thick noncompacted layers). Furthermore, this singular LVHT was confirmed in 3 explanted hearts (figure 2).

Among the total cohort of 20 individuals, median age at diagnosis was 37 [23.7-52.7] years and 12 (60%) were male. HCM was more frequent (13; 65%) than RCM (4; 20%), and 15 individuals (75%) showed a saw-tooth appearance. A total of 16 individuals (80%) showed marked diastolic dysfunction (grade II or III) and 10 (50%) had atrial fibrillation, sometimes in adolescence or early adulthood.

Patients HCM showed an increased interventricular septum (14.3 ± 7 mm), a dilated left atrium (45.6 ± 10.4 mm) and an initially preserved left ventricular ejection fraction (58.5 ± 10.3%). A total of 2 individuals from family A and 2 from family C had bicuspid aortic valve. In addition, 9 patients underwent cardiac magnetic resonance with late gadolinium enhancement assessment, but none of them showed late gadolinium enhancement scar. All of them exhibited an abnormal electrocardiogram: 5 showed T wave inversion in precordial leads and 8 in inferior and precordial leads, 5 had right bundle branch block and 2 showed an unspecific intraventricular conduction delay. None of the patients had low voltages or atrioventricular block. Holter monitoring did not identify increased premature ventricular beats but 1 did identify nonsustained ventricular tachycardia. None of them had symptoms, signs, or a history of skeletal myopathy (mean creatine kinase level 137 ± 58 U/L). Cascade genetic screening showed mild cosegregation of 6 variants with the phenotype (families A, C, D, H, J, K; figure 3), while the remaining 5 cases exhibited a *de novo* presentation (table 1, figure 2 of the supplementary data, table 4 of the supplementary data). Noncarriers showed manifestations of cardiomyopathy.

The remaining 10 families identified with *FLNC*-mRod2 variants without the saw-tooth appearance consisted of 4 obstructive HCM (1 with LVHT but no saw-tooth trait) patients, 1 HCM on postmortem analysis, 1 apical HCM, 1 RCM and 3 individuals without cardiomyopathy.

Table 1
Clinical characteristics of evaluated carriers

Patient	Sex	Age at Dx	*FLNC* variant	Phenotype	CK, U/L	AF	LV thickness, mm	LVEF, %	Diastolic dysfunction	Outcome
Family A										
I.1	M	30	Gly2002Glu	HCM	158	(-)	26	48	Grade III	HF death
II.1*	F	16	Gly2002Glu	HCM+LVHT	164	(-)	15	63	Grade II	(-)
II.2	M	13	Gly2002Glu	HCM+LVHT	185	(-)	32 (Z-s 12.22)	60	Grade II	SVT App ICD shock
Family B										
III.3*	F	15	Gly2011Ar	RCM+LVHT	142	+	7	61	Grade II	HF NYHA II
Family C										
II.1	F	39	Gly2320Ar g	HCM	n/a	+	16	61	Grade II	HF NYHA II
III.1*	M	4	Gly2320Ar g	RCM+LVHT	134	+	7 (Z-s 12.22)	58	Grade III	HTx
III.2	F	5	Gly2320Ar g	RCM+LVHT	72	+	7 (Z-s 12.12)	48	Grade III	HTx
Family D										
II.1*	F	41	Glu2334Lys	HCM+LVHT	84	+	15	66	(-)	HF NYHA II
I.1	M	66	Glu2334Lys	HCM	n/a	+	14	50	Grade III	HF NYHA III
Family E										
II.1*	M	1	Arg2340Trp	HCM+LVHT	320	(-)	13 (Z-s 15.81)	62	Grade II	HF NYHA II NSVT
Family F										
II.1*	M	25	Glu2334Lys	RCM+LVHT	160	+	12	64	Grade III	HTx
Family G										
II.2*	M	1	Pro2301Leu	RCM+LVHT	n/a	(-)	8 (Z-s 13.54)	74	Grade II	(-)
Family H										
III.1*	F	1	Gly2011Ar	HCM+LVHT	70	(-)	14 (Z-s 16.15)	55	Grade II	HF NYHA II
II.2	M	36	Gly2011Ar g	HCM+LVHT	111	(-)	20	64	Grade III	HF Death SVT App ICD shock
III.3	F	6	Gly2011Ar g	HCM+LVHT	50	(-)	7 (Z-s 11.93)	70	(-)	(-)
Family I										
I.1*	M	60	Thr1823Ala	HCM+LVHT	102	+	21	42	Grade III	HF NYHA II Stroke
Family J										
III.5	M	48	Ser1955Leu	HCM	202	+	14	65	Undetermined	(-)
III.3*	M	29	Ser1955Leu	RCM+LVHT	234	(-)	9	53	Grade II	(-)
Family K										
II.1*	M	72	Ala2510Val	HCM	86	+	22	70	Grade II	HF death
III.2	F	52	Ala2510Val	LVHT	n/a	(-)	7	80	(-)	(-)

AF, atrial fibrillation; App, appropriate; CK, creatin kinase (reference values 11-145 U/L); dx, diagnostic; F, female; HCM, hypertrophic cardiomyopathy; HF, heart failure; HTx, heart transplant; ICD, implantable cardioverter-defibrillator; IVS, interventricular septum; LV, left ventricle; LVEF, left ventricular ejection fraction; LVHT, left ventricular hypertrabeculation; M, male; NSVT, nonsustained ventricular tachycardia; NYHA, New York Heart Association; RCM, restrictive cardiomyopathy; VT, sustained ventricular tachycardia; n/a, not available; (+), present; (-), not present.
* Index patients.

Events

After a median follow-up of 6.49 [3.8-21.33] years after phenotype diagnosis, 11 (55%) patients showed symptomatic heart failure (HF) New York Heart Association (NYHA) ≥ II, with 3 of them requiring 3 a heart transplant due to advanced HF in their thirties. Three patients (15%) died from HF. Furthermore, 4 (26.6%) patients had syncope during follow-up and 2 had sustained ventricular tachycardia (SVT) and received an implantable cardioverter-defibrillator (ICD).

Genetic variants

Figure 4 represents the location of the 9 rare variants identified in the *FLNC* ROD2 domain. All the missense variants observed in this cohort were located in the ROD2 domain, specifically in 18 to 21 Ig-like domains. All identified variants were absent in control population databases and bioinformatics predictors showed that they were likely deleterious. ACMG classification identified 4 variants as likely pathogenic and 5 as variants of unknown significance (tables 5 and 6 of the supplementary data). A second

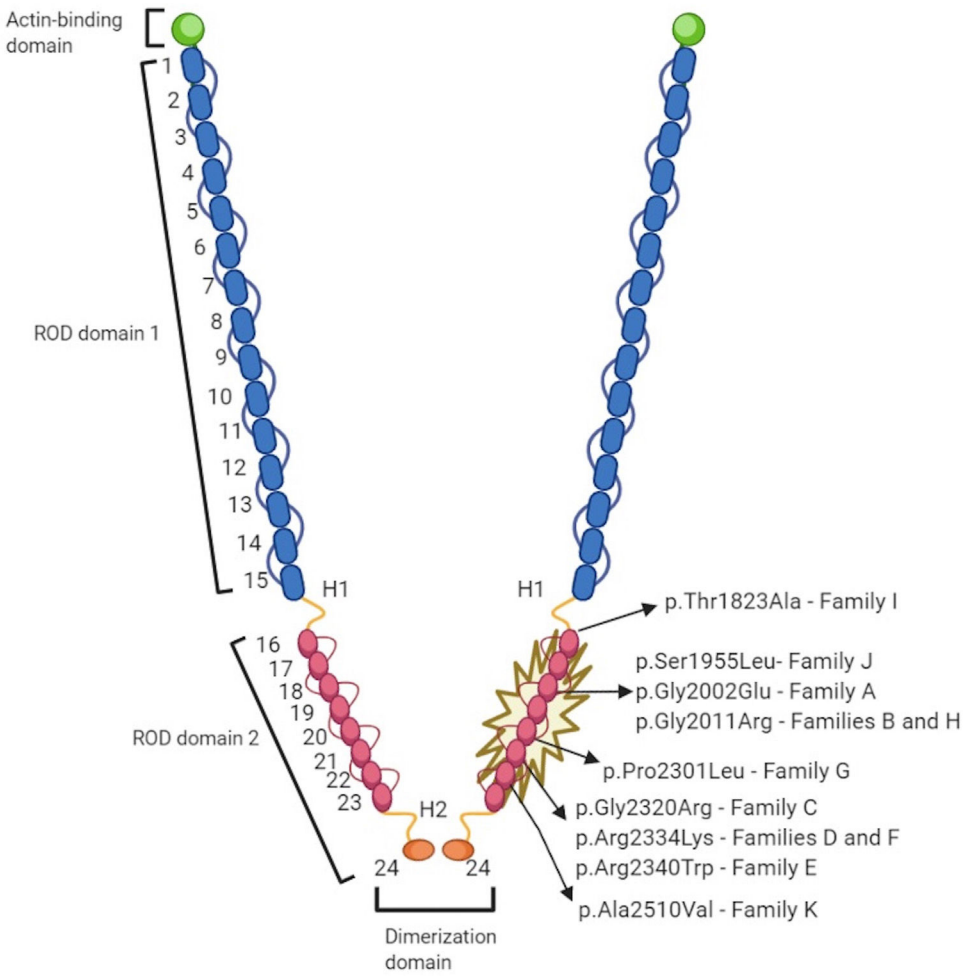

Figure 4. Representative illustration of the FLNC protein with the localization of included *FLNC* variants.

relevant-causative genetic variant was not identified in any of the probands, and paternity was confirmed in 4 of the *de novo* cases. No CNVs were detected in the selected cohort. In all these cases, the quality of the sample was adequate to carry out this analysis.

Histology, histochemistry, and immunohistochemistry

Hematoxylin-eosin staining revealed moderately larger cardiac cells in *FLNC*-tv heart samples compared with *FLNC*-mRod2 and controls (figure 5A). It also revealed a lower density of myofibrils and a slight decrease in intercellular space in *FLNC*-mRod2-affected tissues, resulting in a more compact tissue organization pattern in these specific samples (figure 5B). These results were confirmed by quantitative histological analyses (figure 3 of the supplementary data). The immunohistochemical analysis of *FLNC* confirmed the intracellular localization of this protein in all samples, but in *FLNC*-tv-affected samples, this protein was irregularly distributed and totally absent at the intercalated discs (ID) (figure 5C). In contrast, in *FLNC*-mRod2-affected tissues, it was present within the contractile apparatus, such as in the control group, but it was particularly positive at the ID level.

On the other hand, the—remodeling analysis revealed fibrotic changes in genetically affected samples vs the control (figure 5D), showing a clear increase in fibrillar collagen fibers. In *FLNC*-mRod2-affected samples, we observed this increase in collagen fibers around the cardiomyocytes, exhibiting a well-defined and compacted pattern, different to that observed for *FLNC*-tv (abundant and irregularly organized) (figure 5E-F). Finally, the fibrotic process was semiquantitatively confirmed, showing that the increased collagen content reached 49.2 ± 7.9% in *FLNC*-tv followed by 29 ± 2.5% in *FLNC*-mRod2 genetically affected samples, both being considerably higher than the 26.5 ± 2.2% collagen content observed in the control (figure 3 of the supplementary data). Moreover, the remodeling of the collagen network—fibrotic response—was accompanied by an alteration of the reticular fibers and acid proteoglycans content, intensity, and pattern (figure 4 of the supplementary data). All these histological findings in *FLNC*-mRod2-affected samples were consistent in the 3 samples.

Functional analyses

HT1080 and H9C2 cells were transfected with expression plasmids for wild-type and mutant *FLNC* (p.P2301L, p.E2334K and p.R2340W). Confocal analyses revealed a comparable cellular localization of wild-type and mutant *FLNC* in transfected cells (figure 6 and figure 5 of the supplementary data) indicating that pathogenic protein aggregation was unlikely for the described missense variants.

DISCUSSION

Recently, sporadic *FLNC* missense variants have been described associated with the development of RCM.[4–6] It had also been

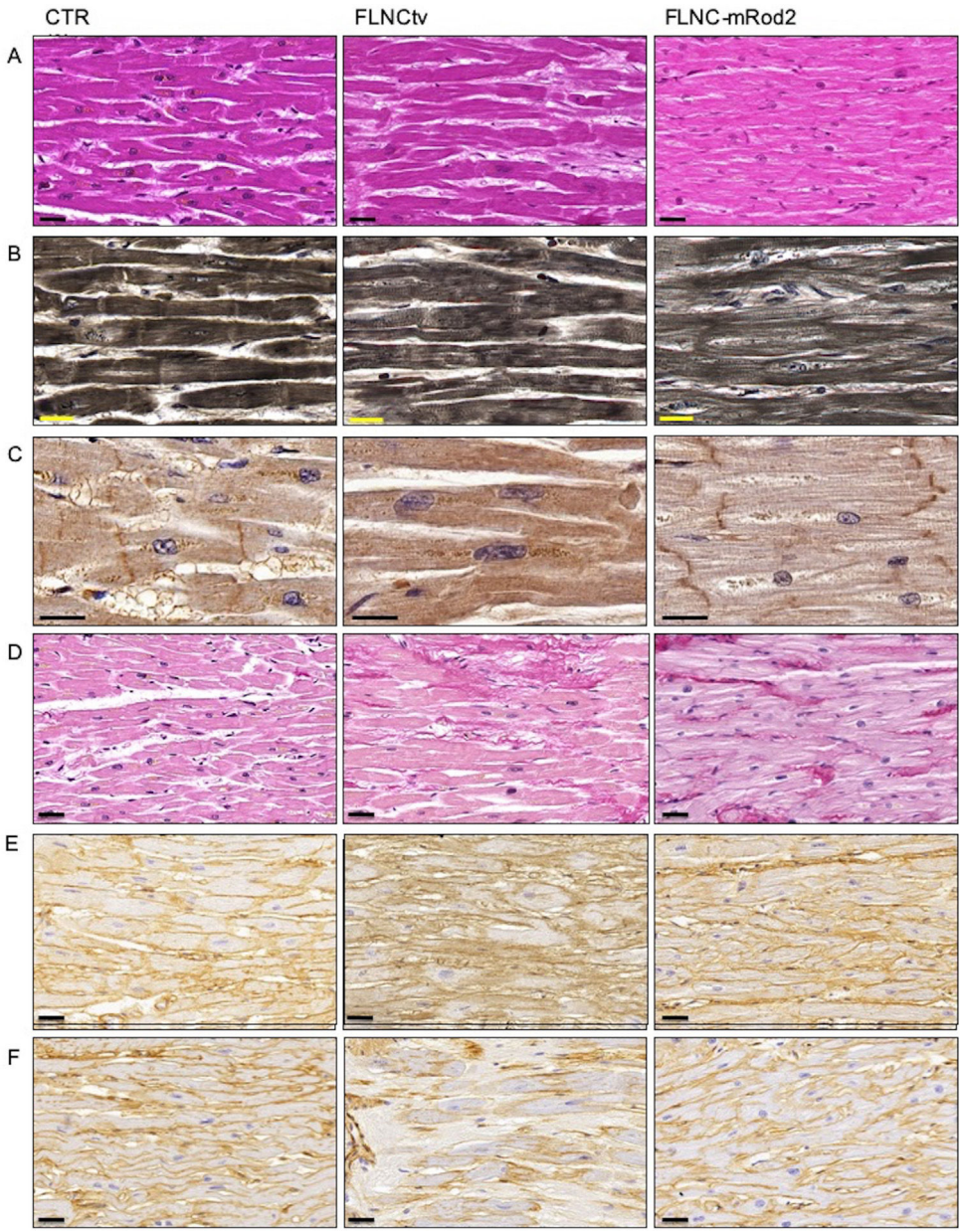

Figure 5. Histological pattern, myofibril histochemistry, *FLNC* immunohistochemistry and ECM remodeling analyses in *FLNC* genetically affected heart tissues. A, hematoxylin-eosin staining of control and genetically compromised heart tissue samples (*FLNC*-tv and *FLNC*-mRod2) showing the increase in the intercellular space in *FLNC*-tv and compaction in *FLNC*-mRod2. B, Heideinhain's hematoxylin for myofibrils demonstrating the minor density in *FLNC*-mRod2. C, Intracellular distribution of *FLNC* as determined by immunohistochemistry. Note the absence of *FLNC* in the intercalated disc of the *FLNC*-tv sample. D, Histochemical identification of fibrillar collagens by Picrosirius staining (in red) with an increase in these fibers in genetically affected samples. Immunohistochemical identification of collagen type I (E) and type IV (F). Scale bar: 20 μm. CTR, control; *FLNC*-mRod2, missense variant in *FLNC*-Rod2 domain; *FLNC*-tv, filamin C truncating variant.

postulated to be associated with HCM.[7] Nevertheless, evidence comes from limited publications. Here we describe for the first time a distinctive cardiac phenotype in a multicenter cohort of patients with rare missense variants at the ROD2 domain of the *FLNC* gene, consisting of a severe HCM/RCM phenotype with an unusual saw-tooth LVHT. The HCM and RCM overlap has previously been described in the context of mutations in cardiac sarcomere protein genes.[21] However, few cases of saw-tooth myocardium have been published to date and none have been associated with a specific gene.[22] Interestingly, most of the patients exhibited the saw-tooth appearance on cardiovascular imaging and some exhibited it at young age. Although both saw-tooth myocardium and NCCM may be considered epiphenomena in the context of another condition, 3 isolated reports of individual patients have suggested a link between NCCM and missense mutations in *FLNC*.[1,23,24] Although saw-tooth patients exhibited deep myocardial recesses, in all patients there was a single and compacted myocardial layer, rather than 2 distinct layers. Therefore, current diagnostic NCCM criteria were not applicable. Interestingly, Roldán-Sevilla et al.[6] described an individual with the p.Pro2301Leu variant, like patient from family G, with RCM in the absence of LVHT. Although phenotypic description is succinct, this difference with our patient may be explained by the already known pleiotropic expression of *FLNC*.[1]

Regarding the clinical impact of *FLNC*-mRod2 variants, most individuals had HF symptoms and marked diastolic dysfunction. It is noticeable that in this small cohort of mostly young patients, there was a high incidence of major clinical events. This is in line

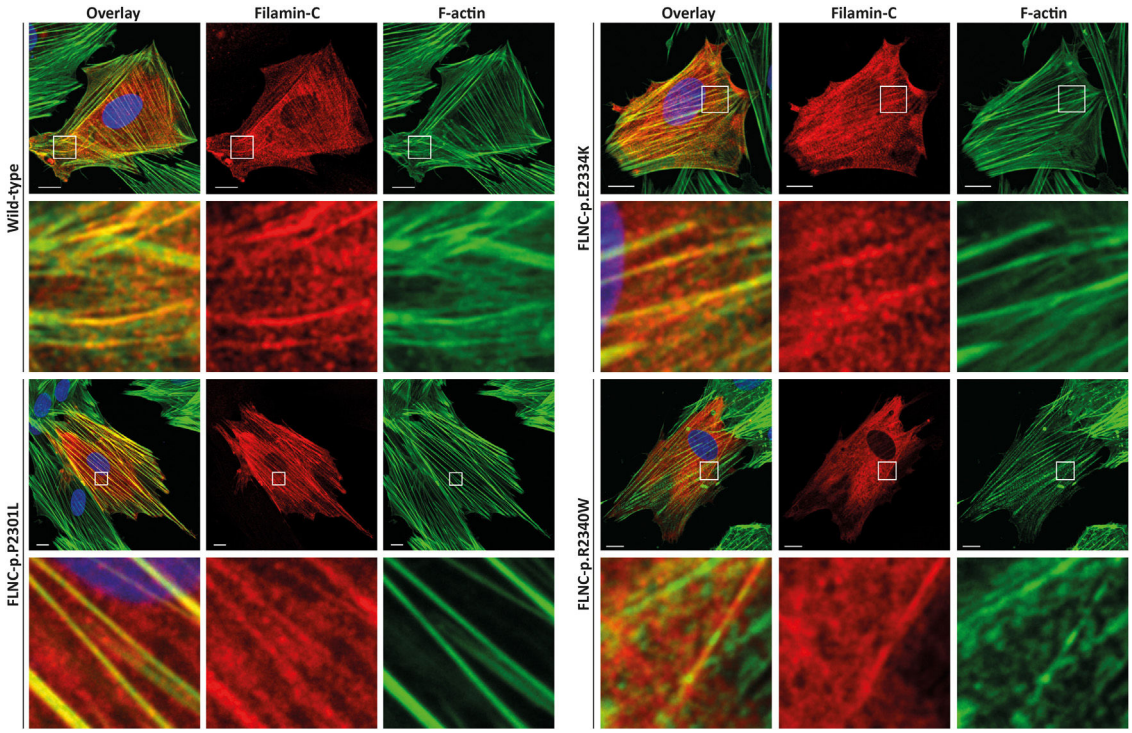

Figure 6. H9C2 cells were transfected with expression plasmids for wild-type and mutant filamin C (p.P2301L, p.E2334K and p.R2340W). c-Myc tagged filamin C is shown in red. F-actin (green) was contained using phalloidin conjugated with Alexa-488. Representative cell images are shown. Scale bars = 10 μm.

with a more severe form of cardiomyopathy than classic HCM and similar to HCM due to mutations in thin filament protein genes such as troponin T.[25] This finding might reveal that restrictive physiology and advanced HF in *FLNC*-mRod2 variants may be common at early stages of the disease, similarly to previous descriptions of patients with advanced HF at young ages.[4,6] Interestingly, we observed a high incidence of *de novo* variants, which supports the likelihood of pathogenicity of the rare variants. Since paternity was confirmed in 4 variants, these are classified as likely pathogenic according to ACMG.[18]

In addition, we have shown evidence of a mild phenotype-genotype cosegregation in 4 independent families, a critical fact that reinforces pathogenicity. *FLNC* is a homodimeric protein encoded by the *FLNC* gene (7q32), composed by 47 coding exons. The protein is composed of an amino-terminal actin-binding domain and a ROD of 24 Ig-like domains which are connected by flexible hinge regions between domains 15 and 16 (hinge 1) and domains 23 and 24 (hinge 2).[26] However, *FLNC* variants have been described as being spread all along the gene, and genotype-phenotype information and cardiac involvement is incomplete; previous reports have questioned the clinical severity, or even the pathogenicity, of common *FLNC* variants in classic forms of HCM, cases that are clearly different to those presented in our cohort[27]: all of our probands carried a missense mutation located at the same ROD2 subdomain, specifically affecting Ig-like domains from 18 to 21 (d18-21), and most of them shared this singular "saw-tooth myocardium" phenotype. The 2 domain pairs (18-19 and 20-21) are preserved in all vertebrate filamins.[28] This ROD2 zone contains the domain responsible for the binding of membrane glycoproteins and it forms a semiflexible ROD with 2 hinge regions and 24 highly homologous tandem repeats, formed by 93 to 103 amino acid residues organized as Ig-type domains. Recent data exploring genotype-phenotype correlations among carriers of *FLNC* pathogenic variants suggest a cluster of missense variants in this region and the development of HCM phenotype.[1] This d18-21 cluster interacts with Z-disc proteins, muscle development and contraction-related proteins. Furthermore, it is of special interest because it is a crucial point for protein phosphorylation.[29] It is suggested that this ROD2 subdomain is essential for *FLNC* dimerization and secondary protein structure acquisition.[23] Therefore, missense variants in the ROD2 subdomain may precipitate a misfolded protein and impaired crosslinking leading to sarcomere disarray and mechanotransduction impairment.[23,30] This hypothesis should be confirmed in future studies.

Histologically, we characterized the tissue features of *FLNC*-mRod2 and *FLNC*-tv in heart samples from 3 explanted hearts and 1 case of sudden cardiac death case, respectively. Although they should be interpreted with caution due to the limited sample, the histological and histochemical analyses of the *FLNC-mRod2* patient showed thin cells with a low density of myofibrils, which may be explained by an impaired crosslinking of the structural, contractile, or even anchor membrane-cytoskeletal proteins. Furthermore, we did not observe *FLNC* aggregates in histology or functional experiments. Here, as previously described,[4,7] we used 2 heterologous systems, with the H9C2 cell line being more representative of myocyte physiology. Although abnormal protein has been observed within aggregates in the tissue of *FLNC*-associated HCM and RCM patients,[31] Valdes-Mas[7] and Brodehl[4] have demonstrated that not all cardiomyopathy-associated *FLNC* missense variants induce protein aggregation, eg, the *FLNC*-mRod2 variants p.I2160F or p.V2297 M.[4,5] Interestingly, the absence of aggregates has been described in the cardiac tissue of patients with *FLNC*-tv in the ROD2 domain indicating the lack of an abnormal *FLNC* protein.[23]

We also confirmed the intracellular localization of *FLNC* in all heart samples, but there were differences among them. While *FLNC*-mRod2 showed an intense presence of *FLNC* in the ID, the *FLNC*-tv-affected samples expressed an irregularly distributed

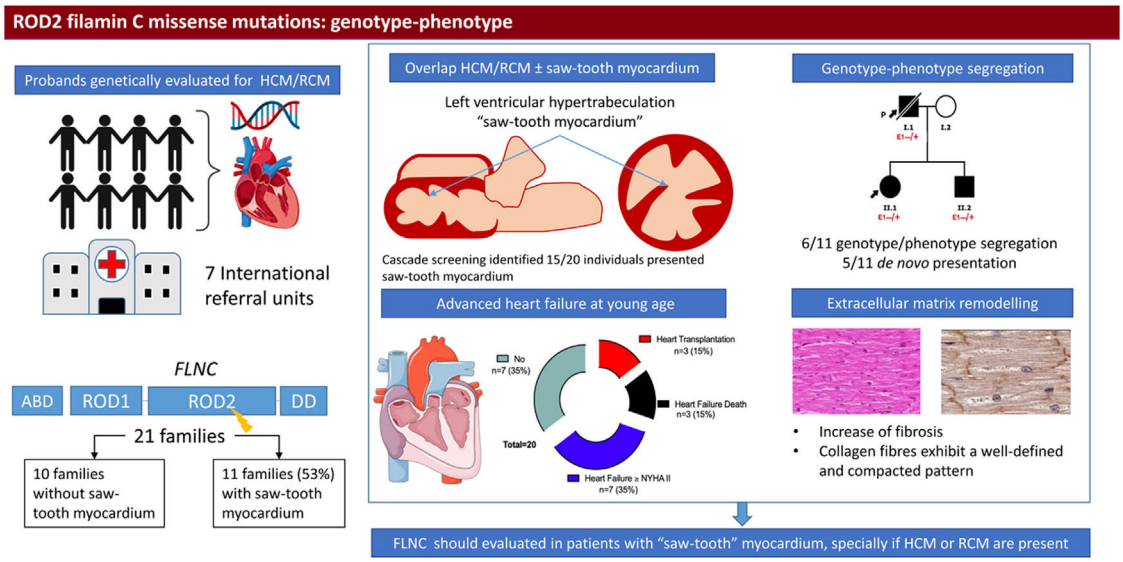

Figure 7. Central illustration. Identification and clinical features of patients with missense variants in the ROD2 domain of *FLNC* and saw-tooth myocardium. We included patients who were genetically evaluated due to hypertrophic cardiomyopathy/restrictive cardiomyopathy and with a missense variant in the ROD2 domain of the *FLNC* gene. Eleven probands exhibited saw-tooth myocardium. Cascade screening identified up to 15 individuals with this trait. In 6 families, we observed mild cosegregation. Patients developed heart failure at a young age. Pathology demonstrated distinct cardiac remodeling. *FLNC*, filamin C; HCM, hypertrophic cardiomyopathy; NYHA, New York Heart Association; RCM, restrictive cardiomyopathy.

protein and was totally absent at the ID level. This absence of *FLNC* at the ID in *FLNC*-tv was previously reported in zebrafish models.[31] Furthermore, we confirmed a different genotype-dependent ECM remodeling leading to diverse fibrotic changes in genetically affected patients. *FLNC*-tv-affected tissues were occupied by an abundant and irregularly organized fibrillar collagen network, confirming an evident fibrotic response.[9] However, the *FLNC*-mRod2-affected samples exhibited a well-defined and compacted tissue pattern with a mild to moderate fibrotic process. This is in contrast with the late gadolinium enhancement results, but may be explained by diffuse myocardial fibrosis that cannot be evaluated by late gadolinium enhancement imaging. Future studies with T_1 mapping would improve interstitial myocardial fibrosis evaluation.

Limitations

The main limitation of this study is the limited number of patients evaluated and its retrospective design. A total of 5 of the 9 rare variants are considered variants of unknown significance, thus limiting the conclusions that can be drawn. For histology, given the nature of the samples, we included only a limited number of independent heart samples affected by this particular genetic condition, limiting the possibility of quantitative and statistical analyses. Cardiac magnetic resonance tissue characterization is limited by the retrospective nature of the study. Furthermore, HT1080 cells may not reproduce human cardiomyocyte physiology.

CONCLUSIONS

Rare missense *FLNC* variants in the ROD2 domain can exhibit an overlapping phenotype comprising HCM and RCM with a saw-tooth LVHT characterized by severe HF progression and distinctive cardiac histopathological remodeling (figure 7).

FUNDING

A. Brodehl is grateful for the financial support of Ruhr-University Bochum (FoRUM, FoRUM-F937R2-2020). Dr Bermúdez Jiménez received funding support by a research training program Río Hortega by Carlos III Institute of Health (CM19/00227).

AUTHORS' CONTRIBUTIONS

All authors made a significant contribution to this work by collecting the cases in their referral centers. F. J. Bermúdez-Jiménez and V. Carriel wrote and coordinated the manuscript equally. AB conducted the functional study. J. Jiménez-Jáimez supervised the clinical and research work and the final version of the manuscript. All authors approved the final version of the manuscript

CONFLICTS OF INTEREST

None.

ACKNOWLEDGMENTS

We would like to thank the patients and their families for their generous and unconditional collaboration. We also thank Fabiola Bermejo Casares, Paloma de la Cueva Batanero (Department of Histology, University of Granada, Spain), Caroline Stanasiuk (EHKI, Germany), Raúl Franco Gutiérrez (University Hospital Lucus Augusti, Santiago de Compostela, Spain), Neus Baena Díez (University Hospital Parc Tauli, Sabadell, Spain), Carlos Gómez Navarro (University Hospital Torrecardenas, Almería, Spain) and Huafrin Kotwal (St. Bartholomew's Hospital, London, UK) for technical assistance. Histological analyses were supported by the Tissue Engineering Group (CTS-115), University of Granada, Spain.

WHAT IS KNOWN ABOUT THE TOPIC?

- FLNC is a striated muscle protein encoded by *FLNC* that serves as a signaling and scaffolding protein.
- *FLNC* gene variants have been strongly associated with arrhythmogenic dilated cardiomyopathy and sporadically with hypertrophic cardiomyopathy, restrictive cardiomyopathy, and noncompaction cardiomyopathy.

WHAT DOES THIS STUDY ADD?

- -This study provides new insight into the spectrum of *FLNC* cardiomyopathy and for the first time describes a novel association with an overlap cardiac phenotype comprising saw-tooth myocardium, hypertrophic and restrictive cardiomyopathy.
- This is the first study to associate a genetic basis with the saw-tooth myocardium pattern.
- The *FLNC* gene should be evaluated among patients with this nonspecific but severe cardiac phenotype for appropriate diagnosis and identification of relatives at risk.

APPENDIX. SUPPLEMENTARY DATA

Supplementary data associated with this article can be found in the online version, at https://doi.org/10.1016/j.rec.2022.08.002

REFERENCES

1. Ader F, De Groote P, Réant P, et al. FLNC pathogenic variants in patients with cardiomyopathies: Prevalence and genotype-phenotype correlations. *Clin Genet.* 2019;96:317–329.
2. Takada F, Vander Woude DL, Tong HQ, et al. Myozenin: An α-actinin- and γ-filamin-binding protein of skeletal muscle Z lines. *Proc Natl Acad Sci U S A.* 2001;98:1595–1600.
3. Selcen D, Engel AG. Myofibrillar myopathies. In: Corrado A, ed. In: *Muscular Dystrophy: Causes and Management.*. New York: Nova Science Publishers, Inc; 2013:247–265.
4. Brodehl A, Ferrier RA, Hamilton SJ, et al. Mutations in FLNC are Associated with Familial Restrictive Cardiomyopathy. *Hum Mutat.* 2016;37:269–279.
5. Tucker NR, McLellan MA, Hu D, et al. Novel Mutation in FLNC (Filamin C) Causes Familial Restrictive Cardiomyopathy. *Circ Cardiovasc Genet.* 2017;10:e001780.
6. Roldán-Sevilla A, Palomino-Doza J, de Juan J, et al. Missense Mutations in the FLNC Gene Causing Familial Restrictive Cardiomyopathy. *Circ Genomic Precis Med.* 2019;12:e002388.
7. Valdés-Mas R, Gutiérrez-Fernández A, Gómez J, et al. Mutations in filamin C cause a new form of familial hypertrophic cardiomyopathy. *Nat Commun.* 2014;5:5326.
8. Waning JI, van. Hoedemaekers YM, Rijdt WPt., et al. FLNC missense variants in familial noncompaction cardiomyopathy. *Cardiogenetics.* 2019;9:8181.
9. Ortiz-Genga MF, Cuenca S, Dal Ferro M, et al. Truncating FLNC Mutations Are Associated With High-Risk Dilated and Arrhythmogenic Cardiomyopathies. *J Am Coll Cardiol.* 2016;68:2440–2451.
10. Gigli M, Stolfo D, Graw SL, et al. Phenotypic Expression. *Natural History and Risk Stratification of Cardiomyopathy Caused by Filamin C Truncating Variants Circulation.* 2021;144:1600–1611.
11. Lang RM, Badano LP, Victor MA, et al. Recommendations for cardiac chamber quantification by echocardiography in adults: An update from the American Society of Echocardiography and the European Association of Cardiovascular Imaging. *J Am Soc Echocardiogr.* 2015;28:1–39e14.
12. Nagueh SF, Smiseth OA, Appleton CP, et al. Recommendations for the Evaluation of Left Ventricular Diastolic Function by Echocardiography: An Update from the American Society of Echocardiography and the European Association of Cardiovascular Imaging. *J Am Soc Echocardiogr.* 2016;29:277–314.
13. Finsterer J, Stöllberger C, Towbin JA. Left ventricular noncompaction. *Nat Rev Cardiol.* 2017;14:224–237.
14. Stenson PD, Ball EV, Mort M, et al. Human Gene Mutation Database (HGMD): 2003 update. *Hum Mutat.* 2003;21:577–581.
15. Landrum MJ, Lee JM, Benson M, et al. ClinVar: public archive of interpretations of clinically relevant variants. *Nucleic Acids Res.* 2016;44:D862–D868.
16. Lek M, Karczewski KJ, Minikel EV, et al. Exome Aggregation Consortium. *Analysis of protein-coding genetic variation in 60706 humans Nature.* 2016;536:285–291.
17. Nyholt DR. All LODs are not created equal. *Am J Hum Genet.* 2000;67:282–288.
18. Richards S, Aziz N, Bale S, et al. Standards and Guidelines for the Interpretation of Sequence Variants: A Joint Consensus Recommendation of the American College of Medical Genetics and Genomics and the Association for Molecular Pathology. *Genet Med.* 2015;17:405–424.
19. Carriel V, Campos F, Aneiros-Fernández J, Kiernan JA. Tissue Fixation and Processing for the Histological Identification of Lipids. *Methods Mol Biol.* 2017;1560:197–206.
20. Carriel V, Garzón I, Campos A, Cornelissen M, Alaminos M. Differential expression of GAP-43 and neurofilament during peripheral nerve regeneration through bioartificial conduits. *J Tissue Eng Regen Med.* 2017;11:553–563.
21. Olivotto I, d'Amati G, Basso C, et al. Defining phenotypes and disease progression in sarcomeric cardiomyopathies: contemporary role of clinical investigations. *Cardiovasc Res.* 2015;105:409–423.
22. Garcia-Pavia P, Dominguez F. Saw-Tooth Cardiomyopathy: Try Not to Stumble Twice Over the Same Stone. *JACC Case Reports.* 2020;2:1210.
23. Verdonschot JAJ, Vanhoutte EK, Claes GRF, et al. A mutation update for the FLNC gene in myopathies and cardiomyopathies. *Hum Mutat.* 2020;41:1091–1111.
24. Miszalski-Jamka K, Jefferies JL, Mazur W, et al. Novel Genetic Triggers and Genotype–Phenotype Correlations in Patients With Left Ventricular Noncompaction. *Circ Cardiovasc Genet.* 2017;10:e001763.
25. Coppini R, Ho CY, Ashley E, et al. Clinical phenotype and outcome of hypertrophic cardiomyopathy associated with thin-filament gene mutations. *J Am Coll Cardiol.* 2014;64:2589–2600.
26. Razinia Z, Mäkelä T, Ylänne J, Calderwood DA. Filamins in Mechanosensing and Signaling. *Annu Rev Biophys.* 2012;41:227–246.
27. Cui H, Wang J, Zhang C, et al. Mutation profile of FLNC gene and its prognostic relevance in patients with hypertrophic cardiomyopathy. *Mol Genet Genomic Med.* 2018;6:1104–1113.
28. Heikkinen OK, Ruskamo S, Konarev PV, et al. Atomic structures of 2 novel immunoglobulin-like domain pairs in the actin crosslinking protein filamin. *J Biol Chem.* 2009;284:25450–25458.
29. Reimann L, Schwäble AN, Fricke AL, et al. Phosphoproteomics identifies dual-site phosphorylation in an extended basophilic motif regulating FILIP1-mediated degradation of FLNC. *Commun Biol.* 2020;3:253.
30. Mao Z, Nakamura F. Structure and function of filamin c in the muscle z-disc. *Int J Mol Sci.* 2020;21:2696.
31. Begay RL, Tharp CA, Martin A, et al. FLNC Gene Splice Mutations Cause Dilated Cardiomyopathy. *JACC Basic to Transl Sci.* 2016;1:344–359.